

## CALIBRATING NEBULAR DIAGNOSTICS OF $T_\star$ AND ABUNDANCE

M. S. Oey,<sup>1,2</sup> J. C. Shields,<sup>3</sup> M. A. Dopita,<sup>4</sup> and R. C. Smith<sup>5</sup>

### RESUMEN

Hicimos espectroscopía de regiones H II en la LMC con poblaciones estelares clasificadas, lo que nos permite restringir los parámetros de la fotoionización. Evaluamos, usando modelos de fotoionización, los diagnósticos de  $T_\star$  y abundancias. Incluimos el cociente  $[\text{Ne III}]/\text{H}\beta$  como un diagnóstico de  $T_\star$ . El cociente  $[\text{Ne III}]/\text{H}\beta$  tiene una mayor sensibilidad a las estrellas O tempranas que el comunmente usado parámetro  $\eta'$ , también es menos afectado por la morfología y la presencia de choques. Presentamos una calibración preliminar para los diagnósticos de  $T_\star$  con la metalicidad de la LMC. También introducimos  $S_{234} \equiv ([\text{S II}] + [\text{S III}] + [\text{S IV}])/\text{H}\beta$  como un diagnóstico para la abundancia de S.  $S_{234}$  es mucho menos sensible al parámetro de ionización que  $S_{23}$  o  $R_{23}$ . La intensidad de  $[\text{S IV}] 10.5 \mu\text{m}$  es fácilmente estimada de los cocientes de líneas de óptico a IR medio. Presentamos calibraciones de  $S_{23}$  y  $S_{234}$  que sirven para metalicidades  $Z \lesssim 0.5Z_\odot$ .

### ABSTRACT

We obtained nebular spectroscopy of LMC H II regions having classified stellar populations, thereby strongly constraining the ionization input parameters. Using photoionization models, we then evaluate the performance of nebular diagnostics of  $T_\star$  and abundance. We introduce  $[\text{Ne III}]/\text{H}\beta$  as a nebular diagnostic of the ionizing stellar  $T_\star$ . In contrast to the widely-used  $\eta'$  parameter,  $[\text{Ne III}]/\text{H}\beta$  has greater sensitivity to mid and early O-stars, and is robust to nebular morphology and the presence of shocks. We present a preliminary calibration of both  $T_\star$  diagnostics for LMC metallicity. We also introduce  $S_{234} \equiv ([\text{S II}] + [\text{S III}] + [\text{S IV}])/\text{H}\beta$  as a diagnostic of S abundance.  $S_{234}$  is much less sensitive to the nebular ionization parameter than is  $S_{23}$  or  $R_{23}$ . The intensity of  $[\text{S IV}] 10.5 \mu\text{m}$  is easily estimated from the optical and near-IR line ratios. We present calibrations of  $S_{23}$  and  $S_{234}$  that are reliable at metallicities  $Z \lesssim 0.5Z_\odot$ .

*Key Words:* GALAXIES: ABUNDANCES — H II REGIONS — MAGELLANIC CLOUDS — STARS: FUNDAMENTAL PARAMETERS — SUPERNOVA REMNANTS

### 1. INTRODUCTION

Nebular emission-line diagnostics are one of our most important probes of conditions in extragalactic star-forming regions. In particular, these diagnostics are a primary means of constraining ionizing stellar populations and metallicities in distant galaxies. However, we rely heavily on photoionization models to interpret observed nebular emission-line ratios, and comparisons between theoretical models and observations have been lacking, especially for ordinary H II regions. Therefore, we have obtained long-slit spectroscopic observations of four H II regions in the Large Magellanic Cloud (LMC), for the purpose of comparing the observed emission-line diagnostics with predictions from photoionization models. The sample spans a range in stellar spectral type from O7 to WNE, and in nebular morphology from classical Strömgren sphere to extreme shell. Two objects show evidence of shock excitation.

We obtained both stationary, spatially-resolved observations of these nebulae, and scanned, spatially-integrated observations. A complete investigation of the entire dataset is presented by Oey et al. (2000; Paper I) and Oey & Shields (2000; Paper II). The spatially resolved observations generally showed excellent agreement between photoionization models and observations. However, a puzzling exception was our finding that the temperature-sensitive ratio  $[\text{O III}] \lambda 4363/\lambda 5007$  is *over*predicted by the models (Paper I). This is opposite to the expected effect of electron temperature fluctuations (Peimbert 1967). Our investigation of the abundance determinations shows that it is essential to use an appropriate relation between the electron temperatures in the high and low ionization zones, which could otherwise introduce errors in the abundance determinations of up to 0.2 dex. Interestingly, we find no evidence of abundance variations in DEM L199, a large H II complex dominated by three early-type WR stars. For further details on our results from the spatially resolved data, we refer the reader to Papers I and II. Below, we summarize results from

<sup>1</sup>Space Telescope Science Institute, USA (STScI Fellow).

<sup>2</sup>Present address: Lowell Observatory, Flagstaff, USA.

<sup>3</sup>Ohio University, USA. <sup>4</sup>ANU, Australia.

<sup>5</sup>Cerro Tololo Inter-American Observatory, Chile.

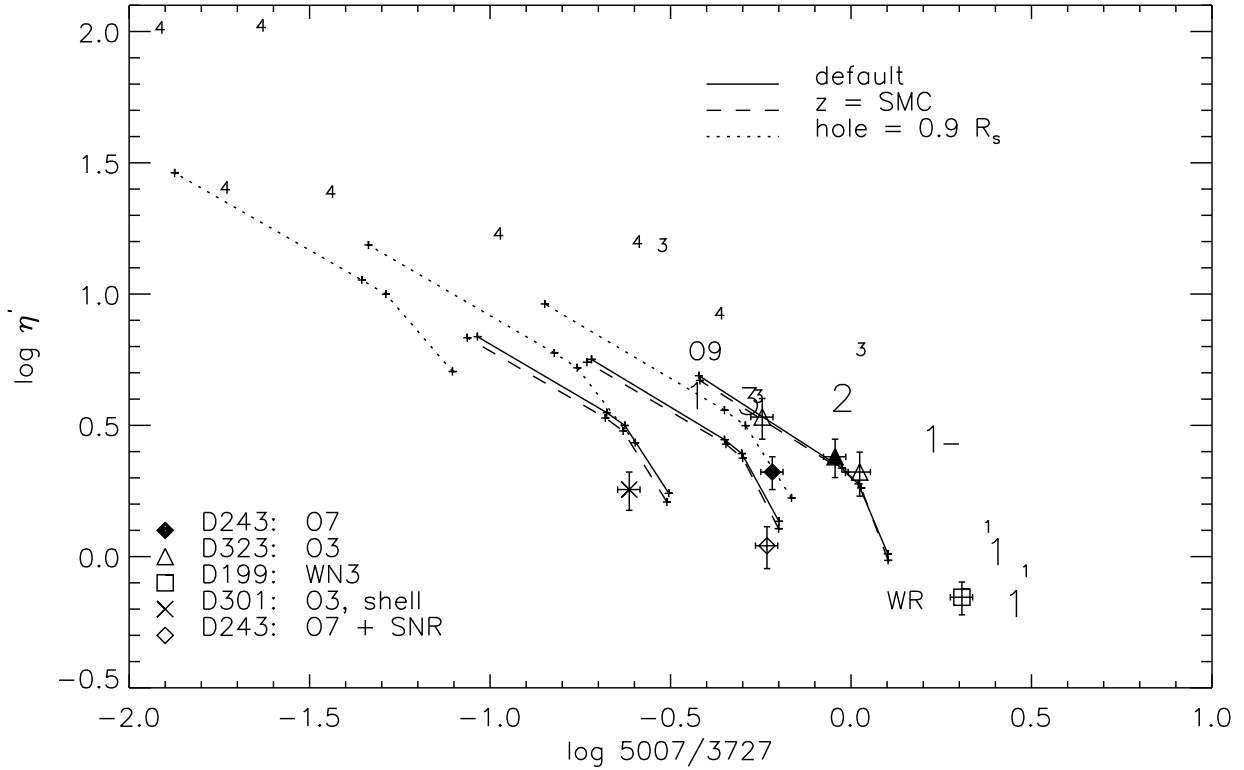


Fig. 1. Model photoionization tracks for  $\eta'$  vs  $[\text{O III}]/[\text{O II}]$ , using WR, O3, O7, and O9 stellar atmospheres. Symbols show our data, and numerals show nebular data from the Kennicutt et al. (2000) sample, with ionizing stellar spectral types binned according to the key; objects along the bottom are non-detections. See text for more details.

the spatially-integrated observations, which resemble those that would be obtained if the LMC were at a distance of 15–20 Mpc.

## 2. DIAGNOSTICS OF $T_*$

### 2.1. The $\eta'$ Parameter

The most widely-used diagnostic of  $T_*$  has been the “radiation softness parameter” of Vázquez & Pagel (1988), defined as the relative ratios of singly to doubly-ionized O and S.

$$\eta' \equiv \frac{[\text{O II}] \lambda 3727 / [\text{O III}] \lambda \lambda 4959, 5007}{[\text{S II}] \lambda 6724 / [\text{S III}] \lambda \lambda 9069, 9532}. \quad (1)$$

Figure 1 shows theoretical tracks of  $\eta'$  vs.  $[\text{O III}]/[\text{O II}]$ , with our spatially integrated observations overplotted. The models are generated with the photoionization code MAPPINGS II (Sutherland & Dopita 1993), using stellar atmospheres from Schaerer & de Koter (1997) and Schmutz, Leitherer, & Gruenwald (1992). The default models (solid lines) have LMC metallicity and central hole size of 0.1 times the Strömgren radius ( $R_s$ ). The three tracks have electron density varying between

1, 10, and 100  $\text{cm}^{-3}$ , which are directly proportional to variations in the ionization parameter  $U$ , with increasing  $U$  corresponding to increasing  $\log [\text{O III}]/[\text{O II}]$ . The individual models represent spectral types of roughly O9, O7, O3, and early WR, toward decreasing values of  $\eta'$ , respectively. We also show model tracks for a shell morphology having an inner radius of 0.9  $R_s$  (dotted lines), and tracks having SMC metallicity but otherwise the same as the default. The data points for our sample of LMC nebulae are plotted with symbols identified in the key. Numerals show objects from the Kennicutt et al. (2000) sample, with large and small numerals indicating LMC and Galactic objects, respectively; these data are not spatially integrated over the entire nebulae (see Paper I).

For both the models and data, Figure 1 shows that  $\eta'$  can effectively discern the presence of WR stars and late-type O stars. However, mid- and early-type O stars yield highly degenerate values of  $\eta'$ . Thus, this diagnostic is essentially insensitive to  $T_* \gtrsim 40,000$  K, with the exception of the WR stars. In addition, Figure 1 shows that  $\eta'$  is also sensitive to

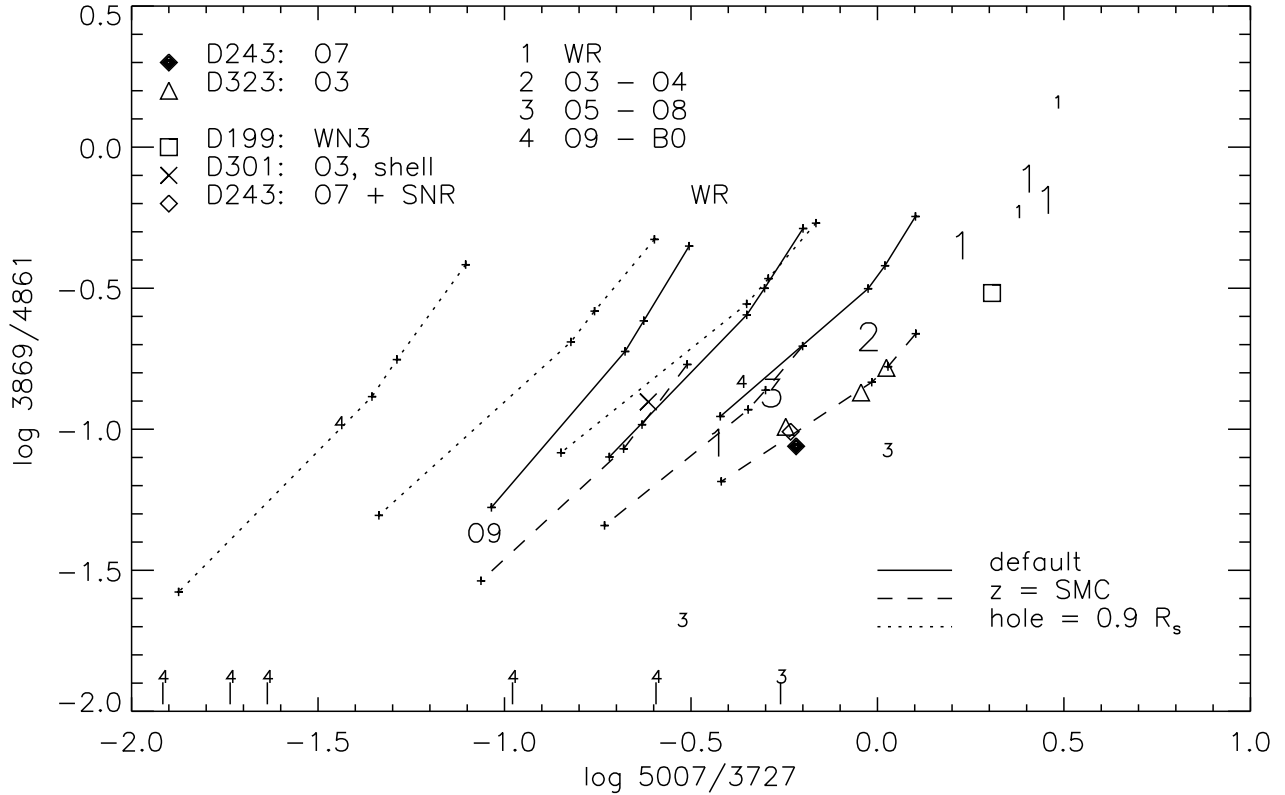


Fig. 2. Same as Figure 1 for  $[\text{Ne III}]/\text{H}\beta$  vs  $[\text{O III}]/[\text{O II}]$ .

nebular morphology. The model tracks for a hollow shell structure (dotted lines) are clearly offset from the default models.

Peimbert, Sarmiento, & Fierro (1991) showed that the inclusion of supernova remnants (SNRs) within integrated H II region spectra can affect interpretation of the nebular conditions. The object DEM 243 encompasses a SNR, and Figure 1 shows data points for the H II region both with and without the SNR included (open and solid diamonds, respectively). DEM 301 (cross) also shows evidence of shock excitation (Paper I). It is apparent in Figure 1 that the  $\eta'$  values of DEM 243 with the SNR, and DEM 301, overestimate  $T_*$  in view of the actual stellar spectral types. This therefore shows that  $\eta'$  is also sensitive to the presence of shocks.

### 2.2. The $[\text{Ne III}]/\text{H}\beta$ Parameter

To address these shortcomings in the  $\eta'$  diagnostic, we therefore introduce  $[\text{Ne III}]/\text{H}\beta$  as a complementary diagnostic of  $T_*$ . Although this ratio is sensitive to abundance, the high ionization potential (40.96 eV) for Ne III yields greater sensitivity to hotter ionizing spectral types. Likewise, this high ionization potential reduces sensitivity to shock excitation.

In Figure 2 we show model tracks of  $\log [\text{Ne III}]/\text{H}\beta$  vs  $\log [\text{O III}]/[\text{O II}]$ , for sequences in  $T_*$ , with symbols as in Figure 1. Figure 2 shows that  $[\text{Ne III}]/\text{H}\beta$  is a fairly successful discriminant of  $T_*$ , even between mid and early O-types. The dotted lines also show that it is highly insensitive to nebular morphology. In addition, the two data points for DEM 243 including and excluding the SNR (solid and open diamonds, respectively) now show agreement in  $[\text{Ne III}]/\text{H}\beta$ , demonstrating insensitivity to shocks. This is further supported by the data for DEM 301 (cross), which also falls in the locus expected for its  $T_*$ . Thus,  $[\text{Ne III}]/\text{H}\beta$  holds promise as a useful  $T_*$  diagnostic for hot O stars. Interestingly, the Galactic and LMC objects do not seem differentiated as expected for their different metallicities. Table 1 gives a preliminary empirical calibration for these  $T_*$  diagnostics. Further details can be found in Paper I.

### 3. DIAGNOSTICS OF METALLICITY: $S_{234}$

H II region metallicities are often estimated using the “bright-line” diagnostic of O/H:  $R_{23} \equiv ([\text{O II}] + [\text{O III}])/\text{H}\beta$  (Pagel et al. 1979). Recently, a similar diagnostic has been introduced for S:  $S_{23} \equiv ([\text{S II}] + [\text{S III}])/\text{H}\beta$  (Vílchez & Esteban 1996). Em-

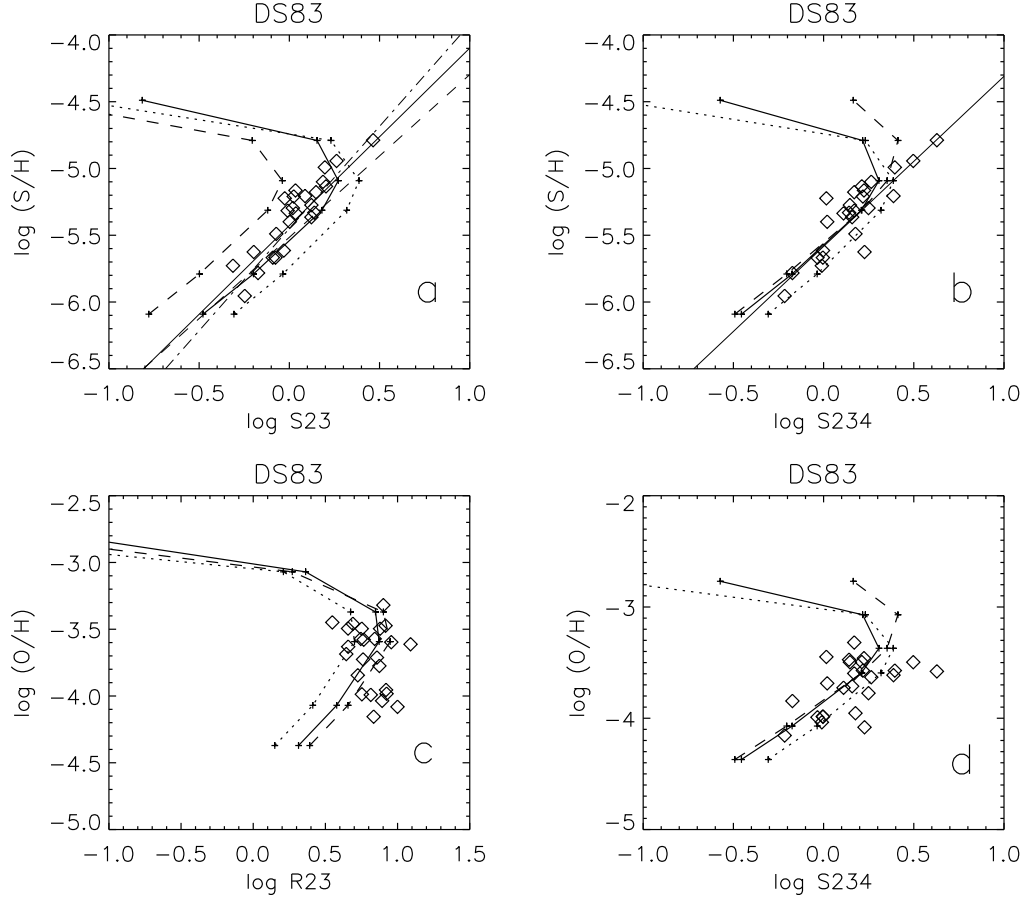


Fig. 3. Theoretical tracks for (a)  $S_{23}$ , (b)  $S_{234}$ , (c)  $R_{23}$ , and (d)  $\log(\text{O}/\text{H})$  vs.  $\log S_{234}$ , computed from models at 0.05, 0.1, 0.3, 0.5, 1.0, and  $2.0Z_{\odot}$ . Dashed, solid, and dotted lines correspond to  $\log U = -2$ ,  $-3$ , and  $-4$ , respectively, and are overplotted with data from Dennefeld & Stasińska (1983). Straight lines are calibrations: solid line is fitted to our models for  $Z \leq 0.5Z_{\odot}$ ; dashed is from Díaz & Pérez-Montero (2000); dash-dot from Christensen et al. (1997).

TABLE 1  
EMPIRICAL CALIBRATION OF  $T_{\star}$   
DIAGNOSTICS<sup>a</sup>

Sp. type	$\log([\text{Ne III}] \lambda 3869/\text{H}\beta)$	$\log \eta'$
WR	$> -0.6$	$< 0.2$
O3–O4	$-0.9$ to $-0.6$	...
O5–O8	$-1.5$ to $-0.9$	...
O9 and later	$< -1.5$	$> 1.0$

<sup>a</sup>For LMC metallicity.

empirical calibrations for  $S_{23}$  have been presented by Christensen, Petersen, & Gammelgaard (1997) and Díaz & Pérez-Montero (2000), who suggested that it would be less  $U$ -sensitive than  $R_{23}$  and would also present a larger dynamic range.

Figure 3 shows theoretical tracks for the abundance diagnostics, using the same photoionization

code and stellar atmosphere models as before. These are overplotted with nebular data points from Dennefeld & Stasińska (1983), who obtained optical and near-IR spectrophotometry of a large sample of nebulae, with electron temperatures derived from the ratio  $\lambda 4363/\lambda 5007$ . Our models show that  $S_{23}$  is actually more sensitive to  $U$  than is  $R_{23}$ . This results from the omission of  $[\text{S IV}]$ , which has roughly the same ionization potential (35 eV) as  $[\text{O III}]$ . The plot in Figure 3a, of  $\log(\text{S}/\text{H})$  vs.  $\log S_{23}$ , shows the large spread in the three tracks. These correspond to  $\log U = -2$ ,  $-3$ , and  $-4$ , with the first having the lowest values of  $S_{23}$ , as expected for a significant population of  $[\text{S IV}]$ . Note that this sequence of tracks is opposite to that for  $R_{23}$  (Figure 3c), which more completely samples the important ions.

We therefore suggest an abundance diagnostic that includes  $[\text{S IV}]$ , to better sample the relevant ions, and thereby improve the effectiveness of the S

diagnostic (Paper II):

$$S_{234} \equiv \left( [\text{S II}] \lambda 6724 + [\text{S III}] \lambda \lambda 9069, 9532 + [\text{S IV}] 10.5 \mu\text{m} \right) / \text{H}\beta. \quad (2)$$

Although  $[\text{S IV}] 10.5 \mu\text{m}$  is a mid-IR line, its intensity can be estimated from a simple relation between optical and near-IR lines, for metallicities  $Z \lesssim 0.5Z_{\odot}$  (Paper II):

$$\log \frac{[\text{S IV}] 10.5 \mu\text{m}}{[\text{S III}] \lambda \lambda 9069, 9532} = -0.984 + 1.276 \log \frac{[\text{O III}] \lambda \lambda 4959, 5007}{[\text{O II}] \lambda 3727}. \quad (3)$$

This relation provides a simple way to estimate  $S_{234}$ . Figure 3b shows  $S_{234}$  for the same dataset, with the intensity of  $[\text{S IV}] 10.5 \mu\text{m}$  computed from equation 2. The theoretical tracks are dramatically less sensitive to  $U$  than for  $S_{23}$ , or even  $R_{23}$  (Figure 3c).

For  $S_{234}$ , a fit to our models gives a theoretical calibration (Figure 3b):

$$\log (\text{S}/\text{H}) = -5.58 + 1.27 \log S_{234}, \quad (4)$$

For  $S_{23}$ , we have a similar theoretical calibration from the models (Figure 3a, straight solid line):

$$\log (\text{S}/\text{H}) = -5.43 + 1.33 \log S_{23}. \quad (5)$$

The dashed and dot-dashed lines in Figure 3a show calibrations from Christensen et al. (1997) and Díaz

& Pérez-Montero (2000) for comparison. Figure 3d shows that caution is necessary in inferring O abundances from the S diagnostics, since apparently there is significant scatter in S/O. Figure 3 also shows that all of these calibrations are reliable only for  $Z \lesssim 0.5Z_{\odot}$ .

We thank Angeles Díaz, Rob Kennicutt, and Fabio Bresolin for providing access to their data in advance of publication. MSO gratefully acknowledges financial support from the conference organizers that enabled her attendance at this celebration.

#### REFERENCES

- Christensen, T., Petersen, L., & Gammelgaard, P. 1997, *A&A*, 322, 41
- Dennefeld, M. & Stasińska, G. 1983, *A&A*, 118, 234
- Díaz, A. I. & Pérez-Montero, E. 2000, *MNRAS*, 312, 130
- Kennicutt, R. C., Bresolin, F., French, H., & Martin, P. 2000, *ApJ*, 537, 589
- Oey, M. S., Dopita, M. A., Shields, J. C., & Smith, R. C. 2000, *ApJS*, 128, 511 (Paper I)
- Oey, M. S. & Shields, J. C. 2000, *ApJ*, 539, 687 (Paper II)
- Pagel, B. E. J., Edmunds, M. G., Blackwell, D. E., Chun, M. S., & Smith, G. 1979, *MNRAS*, 189, 95
- Peimbert, M. 1967, *ApJ*, 150, 825
- Peimbert, M., Sarmiento, A., & Fierro, J. 1991, *PASP*, 103, 815
- Schaerer, D. & de Koter, A. 1997, *A&A*, 322, 598
- Schmutz, W., Leitherer, C., & Gruenwald, R. 1992, *PASP*, 104, 1164
- Sutherland, R. S. & Dopita, M. A. 1993, *ApJS*, 88, 253
- Vílchez, J. M. & Esteban, C. 1996, *MNRAS*, 290, 265
- Vílchez, J. M. & Pagel, B. E. J. 1988, *MNRAS*, 231, 257

M. S. Oey: Lowell Observatory, 1400 W. Mars Hill Rd, Flagstaff, AZ 86001, USA (oey@lowell.edu).

J. C. Shields: Ohio University, Dept. of Physics and Astronomy, Clippinger Research Labs. 251B, Athens, OH 45701, USA (shields@helios.phy.ohiou.edu).

M. A. Dopita: Research School of Astronomy and Astrophysics, Australian National University, Private Bag, Weston Creek P.O., ACT 2611, Australia (Michael.Dopita@mso.anu.edu.au).

R. C. Smith: Cerro Tololo Inter-American Observatory, Casilla 603, La Serena, Chile (csmith@noao.edu).